Evidence of thin-film precursors formation in hydrokinetic and atomistic simulations of nano-channel capillary filling

Evidence of thin-film precursors formation in hydrokinetic and atomistic simulations of nano-channel capillary filling

S. Chibbaro[1(a)], L. Biferale[3], F. Diotallevi[2], S. Succi[2], K. Binder[4], D. Dimitrov[5], A. Milchev[4], S. Girardo[6] and D. Pisignano[6]

[1] *Department of Mechanical Engineering, University of Tor Vergata - via del Politecnico 1, 00133 Rome, Italy, EU*
[2] *Istituto per le Applicazioni del Calcolo, CNR - V.le del Policlinico 137, 00161 Rome, Italy, EU*
[3] *University of Tor Vergata and INFN - via della Ricerca Scientifica 1, 00133 Rome, Italy, EU*
[4] *Institut für Physik, Johannes Gutenberg Universität Mainz - Staudinger Weg 7, 55099 Mainz, Germany, EU*
[5] *Institute for Chemical Physics, Bulgarian Academy of Sciences - 1113 Sofia, Bulgaria, EU*
[6] *CNR, c/o Università degli Studi di Lecce - via Arnesano, 73100 Lecce, Italy, EU*

Abstract – We present hydrokinetic Lattice Boltzmann and Molecular Dynamics simulations of capillary filling of highly wetting fluids in nano-channels, which provide clear evidence of the formation of thin precursor films, moving ahead of the main capillary front. The dynamics of the precursor films is found to obey a square-root law as the main capillary front, $z^2(t) \propto t$, although with a larger prefactor, which we find to take the same value for both geometries under inspection. Both hydrokinetic and Molecular Dynamics approaches indicate a precursor film thickness of the order of one tenth of the capillary diameter. The quantitative agreement between the hydrokinetic and atomistic methods indicates that the formation and propagation of thin precursors can be handled at a mesoscopic/hydrokinetic level, thereby opening the possibility of using hydrokinetic methods to space-time scales and complex geometries of direct experimental relevance.

Micro- and nano-hydrodynamic flows are playing an emerging role for many applications in material science, chemistry and biology, and consequently they cast a pressing demand for a deeper and better understanding of the basic mechanisms of fluid flow at micro- and nano-scales [1–7], as well as for the development of corresponding efficient computational tools. The formation of thin precursor films in capillary experiments with highly wetting fluids (near-zero contact angle) has been reported by a number of experiments and theoretical works [8–12], mostly in connection with droplet spreading experiments. In spite of its conceptual and practical importance, however, much less work has been directed to the study of precursor films for the case of capillary filling. Indeed, this is of great interest because, by forming and propagating ahead of the main capillary front, thin-film precursors may manage to hide the chemical/geometrical details of the nano-channel walls, thereby exerting a major influence on

the efficiency of nano-channel–coating strategies [13,14]. In this realm, the continuum assumption behind the macroscopic description of fluid flow goes often under question, typical cases in point being slip-flow at solid walls and moving contact line of liquid/gas interface on solid walls [1,8]. In order to keep a continuum description at nanoscopic scales and close to the boundaries, the hydrodynamic equations are usually enriched with generalised boundary conditions, designed in such a way as to collect the complex physics of fluid-wall interactions into a few effective parameters. A more radical approach is to quit the continuum level and turn directly to the atomistic description of fluid flows as a collection of moving molecules [15]. This approach is computationally demanding, thus preventing the attainment of space and time macroscopic scales of experimental interest. In recent years, a third, intermediate, alternative is rapidly materialising, in the form of minimal lattice versions of the Boltzmann kinetic equation [16,17]. By definition, such a mesoscopic approach is best suited to situations where

(a)E-mail: sergio.chibbaro@gmail.com; chibbaro@iac.cnr.it

molecular details, while sufficiently important to require substantial amendments of the continuum assumption, still possess a sufficient degree of universality to allow general continuum symmetries to survive, a situation that we shall dub *supramolecular* for simplicity. Lacking a rigorous bottom-up derivation, the validity of the hydrokinetic approach for supramolecular physics must be assessed case by case [18–21]. The aim of this paper is to study another potentially "supramolecular" situation, *i.e.* the formation and propagation of precursor films in capillary filling at nanoscopic scales. We provide quantitative evidences that the formation and propagation of a precursor film is governed by kinetic-hydrodynamical laws, and that the emergent asymptotic dynamics for the head of the film follows a square-root law —in time— as the bulk fluid. Nevertheless, the prefactors of the two behaviours are different, eventually leading to a stable infinitely long thin precursor film ahead of the front. We employ both MD and hydrokinetic simulations, finding quantitative agreement for both bulk quantities and local density profiles, at all times during the capillary filling process. This lends further support to the idea that many supramolecular problems are efficiently handled with mesoscopic/hydrokinetic methods.

In this work, we use the multicomponent LB model proposed by Shan and Chen [22]. This model caters for an arbitrary number of components, with different molecular mass and reads as follows:

$$f_i^k(\vec{x}+\boldsymbol{c}_i\Delta t, t+\Delta t)-f_i^k(\vec{x},t)=-\frac{\Delta t}{\tau_k}[f_i^k(\vec{x},t)-f_i^{k(eq)}(\vec{x},t)],$$
(1)

where $f^k(\boldsymbol{x},t)$ is the probability density function associated with a mesoscopic particle of velocity $\boldsymbol{c}_i$ for the k-th component, τ_k is a mean collision time of the k-th component (Δt being the time step associated with particle free streaming), and $f_i^{k(eq)}(\vec{x},t)$ is the corresponding Maxwell equilibrium function. The interaction force between particles is the sum of a bulk and a wall components

$$\vec{F}_{bk}(\vec{x})=-n_k(\vec{x})\sum_{\vec{x}'}\sum_{\bar{k}=1}^{s}G_{k\bar{k}}n_{\bar{k}}(\vec{x}')(\vec{x}'-\vec{x}),$$

$$\vec{F}_{wk}(\vec{x})=-n_k(\vec{x})\sum_{\vec{x}'}g_{kw}n_w(\vec{x}')(\vec{x}'-\vec{x}),$$
(2)

where n_k is the local density and the interaction matrix $G_{k\bar{k}}$ is symmetric. In our model, $G_{k\bar{k}}=g_{k\bar{k}}$ (for $|\vec{x}'-\vec{x}|=1$); $G_{k\bar{k}}=g_{k\bar{k}}/4$ (for $|\vec{x}'-\vec{x}|=\sqrt{2}$); and 0 otherwise. At the fluid/solid interface, the wall is regarded as a (solid) phase with a constant number density n_w and g_{kw} is the interaction strength between component k and the wall. By adjusting the parameters g_{kw} and n_w, different wettability can be obtained [23]. This approach allows the definition of a static contact angle θ, spanning the entire range $\theta\in[0°:180°]$ [24]. Concerning the MD
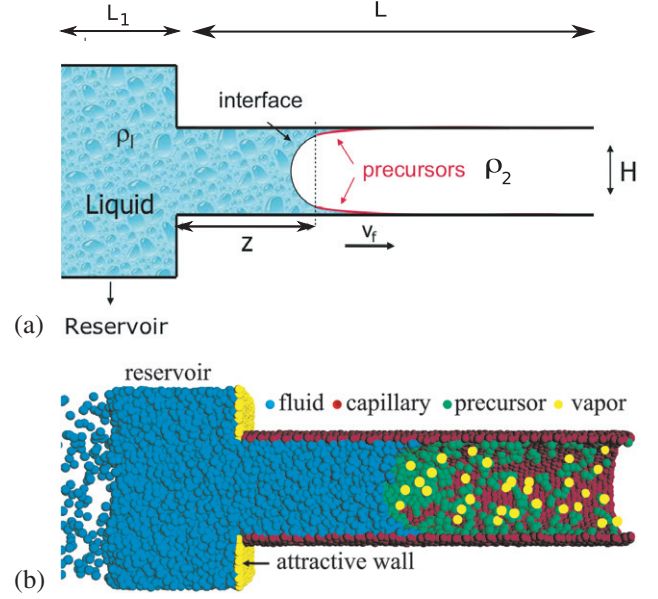

Fig. 1: (Colour on-line) Sketch of the geometry used for the description of the capillary imbibition in the LB and MD simulations. (a) The 2-dimensional geometry, with length $\mathbf{L_1}+\mathbf{L}$ and width H, is divided in two parts. The left part has top and bottom periodic boundary conditions, so as to support a perfectly flat gas-liquid interface, mimicking an "infinite reservoir". In the right half, of length L, there is the actual capillary: the top and bottom boundary conditions are solid walls, with a given contact angle θ. Periodic boundary conditions are also imposed at the inlet and outlet sides. The main LB parameters are: $H\equiv ny\Delta=40$, $\mathbf{L_1}=\mathbf{L}=nz\Delta=170$, $\rho_1=1$; $\rho_2=0.35$, $\mu_1=0.66$, $\mu_2=0.014$, $\gamma=0.016$, where H is the channel height, L is the channel length, $\Delta=1$ is the grid spacing in both directions, ρ_2 and ρ_1 the gas and liquid densities, respectively, μ_k, $k=1,2$ the dynamic viscosities, and γ the surface tension. ny and nz are the number of sites in the lattice, respectively, in the y and z directions. (b) Snapshot of fluid imbibition for MD in the capillary at time $t=1300$ MD time steps. We consider a cylindrical nano-tube of radius $R=10$, whereby the capillary walls are represented by densely packed atoms forming a triangular lattice with lattice constant 1.0 in units of the liquid atom diameter σ. The fluid is in equilibrium with its vapour. Fluid atoms are in blue. Vapour is yellow, tube walls are red and the precursor is green. One distinguishes between vapour and precursor on the basis of the distance of the atoms from tube walls: if a certain particle has no contact with the wall, it is deemed "vapour". The MD parameters are as follows [25]: $R=10\sigma$, $L=80\sigma$, $\rho_l=0.774$, $\mu=6.3$, $\gamma=0.735$, $\sigma=1$, where R is the capillary radius and L its length.

simulation [25], see fig. 1, fluid atoms interact through a LJ potential, $U_{LJ}(r)=4\epsilon[(\sigma/r)^{12}-(\sigma/r)^6]$, where $\epsilon=1.4$ and $\sigma=1.0$. The capillary walls are represented by atoms forming a triangular lattice with spacing 1.0 in units of the liquid atom diameter σ. The wall atoms may fluctuate around their equilibrium positions at $R+\sigma$, subject to a finitely extensible non-linear elastic (FENE) potential

$U_{FENE} = -15\epsilon_w R_0^2 \ln\left(1 - r^2/R_0^2\right)$, $R_0 = 1.5$. Here $\epsilon_w = 1.0 k_B T$, where k_B denotes the Boltzmann constant and T is the temperature of the system; r is the distance between the particle and the virtual point which represents the equilibrium position of the particle in the wall structure. In addition, the wall atoms interact with each other via a Lennard-Jones (LJ) potential which is defined by $\epsilon = \epsilon_{ww} = 1.0$ and $\sigma = \sigma_{ww} = 0.8$ and can be written as $U_{LJww}(r) = 4\epsilon_{ww}[(\sigma_{ww}/r)^{12} - (\sigma_{ww}/r)^6]$. This choice of interactions guarantees no penetration of liquid particles through the wall, and at the same time the mobility of the wall atoms corresponds to the system temperature. The FENE potential acts like an elastic string between the wall particles and their equilibrium positions in the lattice, and keeps the structure of the wall hexagonal. The additional LJ potential attracts neighboring wall particles if they are too far and prevents formation of holes in the wall structure. It is worth emphasizing that we perform MD simulation of a simple generic model on a coarse-grained level, without detailed atomistic description of the fluid and the wall, and we do not take into account electrostatic or other long-ranged interactions. Molecules are advanced in time via the velocity-Verlet algorithm and a dissipative-particle-dynamics thermostat, with friction parameter $\xi = 0.5$, and a thermostat cut-off $r_c = 2.5\sigma$ [15]. The chosen cut-off is larger than the width of the observed precursor and, therefore, we believe that the absence of the complete long-ranged forces is not crucial for the quantitative analysis of the phenomena discussed in the manuscript [26,27]. The integration time step is $\delta t = 0.01 t_0$, where $t_0 = \sqrt{m\sigma^2/48 k_B T} = 1/\sqrt{48}$ is the basic time unit and we have taken the particle mass $m \equiv 1$ and $k_B T \equiv 1$.

We consider a capillary filling experiment, whereby a dense fluid, of density and dynamic viscosity ρ_1, μ_1, penetrates into a channel filled up by a lighter fluid, ρ_2, μ_2, see fig. 1. For this kind of fluid flow, the Lucas-Washburn law is expected to hold, at least at macroscopic scales [28,29] and in the limit $\mu_1 \gg \mu_2$. Recently, the same law has been observed even in nanoscopic experiments [30]. In these limits, the law governing the position, $z(t)$, of the macroscopic meniscus is $z^2(t) - z^2(0) = \frac{\gamma H \cos(\theta)}{C\mu} t$, where γ is the surface tension between liquid and gas, θ is the *static* contact angle, μ is the liquid viscosity, H is the channel height and the factor C depends on the flow geometry (in the present geometry $C_{LB} = 3$; $C_{MD} = 2$). The geometry we are going to investigate is depicted in fig. 1 for both models. It is important to underline that in the LB case, we simulate two immiscible fluids, without any phase transition.

Since binary LB methods do not easily support high-density ratios between the two species, we impose the correct ratio between the two dynamics viscosities through an appropriate choice of the kinematic viscosities. The chosen parameters correspond to an averaged capillary number $Ca \approx 3 \cdot 10^{-2}$ and $Ca \sim 0.1$ for LB and MD respectively.
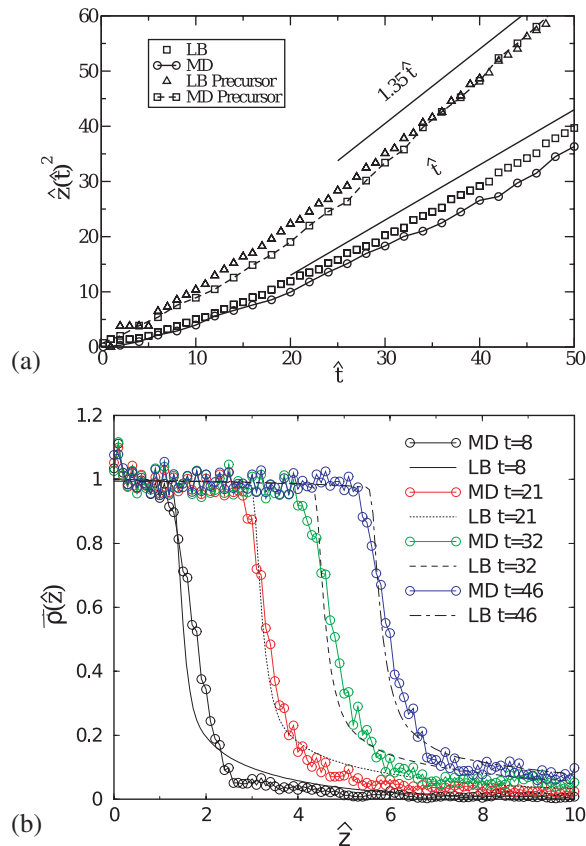

Fig. 2: (Colour on-line) Dynamics of the bulk and precursor meniscus. (a) Position of the liquid meniscus $\hat{z}^2(t)$ for LB and MD simulations. The position of the precursor film, $\hat{z}^2_{prec}(t)$ is also plotted for both models. $\hat{z}_{prec}$ is defined as the rightmost location with density $\rho = \rho_{bulk}/3$. All quantities are given in natural "capillary" units (see text). The asymptotic $(t > 15 t_{cap})$ rise of both precursor and bulk menisci follows a $t^{1/2}$ law, with different prefactors (see the two straight lines), even though the underlying microscopic physics is different. Notably, the precursor film is found to proceed with the law $\hat{z}^2_{prec}(t) = 1.35\hat{t}$. (b) Profiles of the average fluid density $\bar{\rho}(z)$ in the capillary at various times for LB and MD models.

In order to expose the universal character of the phenomenon, results are presented in natural units, namely, space is measured in units of the capillary size, l_{cap} and time in units of the capillary time $t_{cap} = l_{cap}/V_{cap}$, where $V_{cap} = \gamma/\mu$ is the capillary speed and $l_{cap} = H/C_{LB}$ for LB and $l_{cap} = R/C_{MD}$ for MD. In these units, the Lucas-Washburn law takes a very simple universal form

$$\hat{z}^2 = \hat{z}_0^2 + \hat{t}, \qquad (3)$$

where $\hat{z} = z/l_{cap}$, $\hat{t} = t/t_{cap}$ and we have inserted the value of $\cos(\theta) = 1$, corresponding to complete wetting. As to the bulk front position, fig. 2a shows that both MD and LB results superpose with the law (3), while the precursor position develops a faster dynamics, fitted by the relation

$$\hat{z}^2_{prec} = \hat{z}_0^2 + 1.35\hat{t}. \qquad (4)$$

Similar speed-up of the precursor has been reported also in different experimental and numerical situations [10,31]. The precursor is here defined through the density profile, $\overline{\rho}(z)$, averaged over the direction across the channel.

In fig. 2b, we show $\overline{\rho}(z)$ at various instants (always in capillary units), for both MD and LB simulations. The relatively high average density $\overline{\rho}(z)$ near the wall, at later times, witnesses the presence of a precursor film attached to the wall. From this figure, it is appreciated that quantitative agreement between MD and LB is found also at the level of the spatial profile of the density field. This is plausible, since the LB simulations operate on similar principles as the MD ones, namely the fluid-wall interactions are *not* expressed in terms of boundary conditions on the contact angle, like in continuum methods, but rather in terms of fluid-solid (pseudo)potentials (for details see [25]). In fig. 2a, we show the position of the advancing front and the precursor film as a function of time, for both MD and LB simulations. Even though the averaged capillary numbers are not exactly the same, a pretty good agreement between LB and MD is observed. In particular, in both cases, the precursor is also found to obey a $\sqrt{t}$ scaling in time, although with a larger prefactor than the front. As a result, the relative distance between the two keeps growing in time, with the precursors serving as a sort of "carpet", hiding the chemical structure of the wall to the advancing front. As recently pointed out [25,30], our findings indicate that hydrodynamics persists down to nanoscopic scales. The fact that the MD precursor dynamics *quantitatively* matches with mesoscopic simulations, suggests that the precursor physics also shows the same kind of nanoscopic persistence. Concerning the instantaneous interface profile, in fig. 3a we show the structure of the precursor by analysing fluid menisci cuts for different density levels. The agreement between the two methods is again quantitative. In LB, the interface is found to be about 5Δ (leading to the rough estimate, $\Delta \approx 0.2\,\text{nm}$, considering an interface thickness for water/air at room temperature $\Delta\xi \approx 1\,\text{nm}$). The film profile, defined by the isoline at density $\rho = \rho_{bulk}/3$, splits in two regions. In the first one, reaching up to $y \approx 7\Delta = 0.5\hat{\Delta}$, the front is fitted by the expected bulk circle profile. In the second one, extending from $y \approx 7\Delta = 0.5\hat{\Delta}$ to the wall, the film profile is fitted by the analytical expression $\sim Ca^{-1}a^2/z$, where a is a characteristic molecular size, which in our case is set equal to $a = 1$. The analytical profile was proposed for the case of "maximal film" (perfect wetting) [1], under the lubrication approximation, with van der Waals interactions between fluid and walls.

In order to further analyse the previous results, we study the asymptotic case, *i.e.* a situation with a very small fluid velocity (quasi-static), obtained in a longer channel ($L = nz = 1500\Delta$) with the same geometry depicted in fig. 1. To be noted that such domain is too large for an atomistic method and, therefore, we have simulated it with LB only. The results are shown in fig. 3b. In such a case, the departure between the bulk profile and
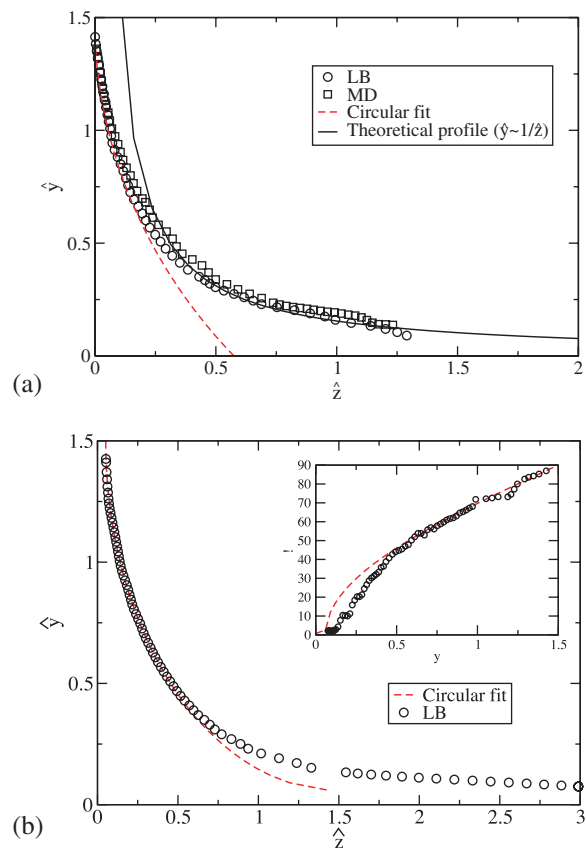

(a)

(b)

Fig. 3: (Colour on-line) Structure of the precursor film. (a) Snapshot of the interface profile for LB and MD models at time $\hat{t} = 20$. Both LB and MD profiles are obtained as isolines at $\rho_{bulk}/\rho = 3$. We also show the circular fit (bold line), valid for the menisci in the bulk region and the $1/z$ profile as suggested by lubrication theory. Notice the clear departure of the interface from a circular fit, due to the different physics close to the wall. Natural "capillary" units are used (see text). Note that, given that MD and LB vertical dimensions are different, MD profiles have been first made dimensionless in natural units and then, for the sake of clarity, rescaled so that the two channel widths superpose. (b) The interface profile at a later stage of capillary filling (symbol: circle). The dashed line corresponds to the circular fit of the bulk ($0.15 < \hat{y} < 1.5$). Notice the long extension of the precursor, here defined as the spatial interval where the profile departs from the circular fit. In the inset, we plot the value of the macroscopic angle defined by the interface curvature at varying distance from the wall.

the precursor shape is even more pronounced, due to the longer elongation of the film close to the wall. In the inset of the same fig. 3b, we also show the macroscopic angle formed by the interface as a function of the distance from the wall. The bulk interface is fitted by a circle extrapolating to the wall with a contact angle $\theta = 0$. It is remarkable that the presence of the precursor film allows the apparent contact angle to vanish less sharply than in the ideal circular case, as visible in the inset of fig. 3b. Moreover, in the inset of fig. 3b the LB curve goes to

zero at a finite value of y, while the circular fit reaches this value for $y = 0$. This is another manifestation of the deviation of the LB profile from the ideal circular case. It is worth noting that there are some small "steps" close to $y = 0$ in the LB profile which are simply due to the discrete interpolation carried out to calculate the value of θ and which disappear increasing the resolution. The deviation from this circular fit is not due to a simple dynamical distortion of the apparent contact angle, since this would lead to an increase of the macroscopic angle. Therefore, this deviation can be interpreted as a signature of the onset of precursor physics [8]. This point is made even clearer by the inset of fig. 3b, where the precursor is associated with the finite part of the fluid with contact angle $\theta = 0$.

Summarising, we have reported quantitative evidence of the formation and the dynamics of precursor films in capillary filling with highly wettable boundaries. The precursor shape shows persistent deviation from an ideal circular meniscus, due to the nanoscopic distortion induced by the interactions with the walls. This is the first time that this diffusive behaviour is observed in capillary filling. This is likely connected to the disjoining pressure induced by van der Waals interactions between fluid and solid [2]. The precursor follows the same square-root law in time as the bulk meniscus, although with a different prefactor, see eq. (4). This prefactor has been found to be the same for both geometries investigated, while its universality with respect to other physical parameters remains to be explored. Our findings are supported by direct comparison between LB, MD simulations and theoretical predictions, which suggests that a hydrokinetic description (LB) together with a proper inclusion of the solid-fluid interaction is able to reproduce this phenomenon.

On the practical side, the hydrokinetic method presented in this work offers the opportunity to perform very efficient numerical simulations of precursor formation and propagation in complex geometries of direct interest for the optimal design of micro- and nano-fluidic devices. In particular, the study of the effect of precursor films in nano-channels with roughness is worthwhile.

$* * *$

REFERENCES

[1] DE GENNES P. G., *Rev. Mod. Phys.*, **57** (1985) 827.
[2] DE GENNES P. G., BROCHARD-WYART F. and QUÉRÉ D., *Bubbles, Pearls, Waves* (Springer) 2003.
[3] BHUSHAN B., ISRAELACHVILI J. N. and LANDMAN U., *Nature*, **374** (1995) 607.
[4] STROOCK A. D. *et al.*, *Science*, **295** (2002) 647.
[5] SUPPLE S. and QUIRKE N., *Phys. Rev. Lett.*, **90** (2003) 214501.
[6] KARABACAK D. M., YAKHOT V. and EKINCI K. L., *Phys. Rev. Lett.*, **98** (2007) 254505.
[7] JOSEPH P. *et al.*, *Phys. Rev. Lett.*, **97** (2006) 156104.
[8] BONN D., EGGERS J., INDEKEU J., MEUNIER J. and ROLLEY E., to be published in *Rev. Mod. Phys.*
[9] PIROUZ KAVEHPOUR H., BEN OVRYN and GARETH H. MCKINLEY, *Phys. Rev. Lett.*, **91** (2003) 196104.
[10] BICO J. and QUÉRÉ D., *Europhys. Lett.*, **61** (2003) 348.
[11] BLAKE T. D. and DE CONINCK J., *Adv. Colloid Interface Sci.*, **96** (2002) 21.
[12] HESLOT F., CAZABAT A. M. and LEVINSON P., *Phys. Rev. Lett.*, **62** (1989) 1286.
[13] COTTIN-BIZONNE S., BARRAT J. L., BOCQUET L. and CHARLAIX E., *Nat. Mater.*, **2** (2003) 237.
[14] TAS N. R. *et al.*, *Appl. Phys. Lett.*, **85** (2004) 3274.
[15] RAPAPORT D., *The Art of Molecular Dynamics Simulations* (Cambridge University Press) 1995.
[16] BENZI R., SUCCI S. and VERGASSOLA, *Phys. Rep.*, **222** (1992) 145.
[17] WOLF-GLADROW D. A., *Lattice-gas Cellular Automata and Lattice Boltzmann Models* (Springer, Berlin) 2000.
[18] HORBACH J. and SUCCI S., *Phys. Rev. Lett.*, **96** (2006) 224503.
[19] SBRAGAGLIA M., BENZI R., BIFERALE L., SUCCI S. and TOSCHI F., *Phys. Rev. Lett.*, **97** (2006) 204503.
[20] SWIFT M. R., OSBORN W. R. and YEOMANS J. M., *Phys. Rev. Lett.*, **75** (1995) 830.
[21] HARTING J., KUNERT C. and HERRMANN H. J., *Europhys. Lett.*, **75** (2006) 328.
[22] SHAN X. and CHEN H., *Phys. Rev. E*, **47** (1993) 1815.
[23] KANG Q., ZHANG D. and CHEN S., *Phys. Fluids*, **14** (2002) 3203.
[24] BENZI R., BIFERALE L., SBRAGAGLIA M., SUCCI S. and TOSCHI F., *Phys. Rev. E*, **74** (2006) 021509.
[25] DIMITROV D. I., MILCHEV A. and BINDER K., *Phys. Rev. Lett.*, **99** (2007) 054501.
[26] MILCHEV A. and BINDER K., *J. Chem. Phys.*, **116** (2002) 7691.
[27] HIROSE K., KONISHO T. and UENO I., *Microgravity Sci. Technol.*, **19** (2007) 81.
[28] WASHBURN E. W., *Phys. Rev.*, **27** (1921) 273.
[29] LUCAS R., *Kolloid-Z.*, **23** (1918) 15.
[30] HUBER P., KNORR K. and KITYK A. V., *Spontaneous Imbibition of Liquids into Nanopores*, in *Dynamics in Small Confining Systems VIII*, edited by FOURKAS JOHN T., LEVITZ PIERRE, OVERNEY RENÉ and URBAKH MICHAEL, *Mater. Res. Soc. Symp. Proc.*, Vol. **899E** (MRS, Warrendale, Penn.) 2006, 0899-N09-07.
[31] POPESCU M. N., DIETRICH S. and OSHANIN G., *J. Phys.: Condens. Matter*, **17** (2005) S4189.